OPTICAL SPECTRA OF LOW-DIMENSIONAL SEMICONDUCTORS

Fu Y Chiragwandi Z Göthberg P Willander M

(Laboratory for Physical Electronics and Photonics, Department of Physics and Engineering Physics, Chalmers University of Technology, S-412 96 Göteborg, Sweden)

Abstract We have studied the optical spectra of low-dimensional semiconductor systems by calculating all possible optical transitions between electronic states. Optical absorption and emission have been obtained under different carrier population conditions and in different photon wavelengths. The line-shapes of the peaks in the optical spectrum are determined by the density of electronic states of the system, and the symmetries and intensities of these peaks can be improved by reducing the dimensionality of the system. Optical gain requires in general a population inversion, whereas for a quantum-dot system, there exists a threshold value of the population inversion.

Key words optical spectrum, low-dimensional semiconductor, optical gain, population inversion.

Introduction

The development of low-dimensional semiconductor materials has been extensive[1]. To a large extent, the modern microelectronics industry is still largely based on the conventional device components (with a reduced discrete device dimension following Moore's law), whereas the components in optoelectronics are already dominated by low-dimensional systems[2]. Light-emitting diodes are extensively applied, quantum-well-based infrared photodetectors have been commercialized[3], vertical-cavity surface-emitting laser (VCSEL) sources have been widely and rapidly adopted in optical communication. With an artificially tailored energy band structure of charged carriers by controlling the dimensionality and geometric shape, low-dimensional system is expected to have superior device characteristics in laser, detection and modulation actions.

Thus far, optical emission and optical absorption have been extensively studied in a separated manner, i.e., optical gain spectrum in laser[14], photoluminescence in material characterization[5], and optical absorption in photodetector[6]. In this work we study the optical properties of low-dimensional systems by calculating their unified optical spectra. The general formulation of the optical spectrum (coefficient) is presented in Section Ⅱ, while condition of optical absorption and emission, and the effects of the system's dimensionality and external carrier injection condition are to be discussed in Section Ⅲ.

1 General Description About Optical Spectrum

We start with the time-dependent Schrödinger equation

$$i\hbar\frac{\partial\psi}{\partial t} = (H + H')\psi, \tag{1}$$

where

$$H = -\frac{\hbar^2\nabla^2}{2m_0} + V(r) - e\phi(r),$$

$$H' = \frac{ie\hbar}{m_0}\mathbf{A}\cdot\nabla. \tag{2}$$

A and ϕ are vector and scalar potentials of the electromagnetic field. $V(r)$ is the lattice potential. The total wavefunction of the perturbed electron system ($H + H'$) is generally expressed as

$$\Psi(r,t) = \sum_i c_i\psi_{k_i}^{(r)}e^{iE_{k_i}t/\hbar},$$

$$H\psi_{k_i}(r) = E_{k_i}\psi_{k_i}^{(r)}. \tag{3}$$

where k is the electron wavevector (for low-dimensional system, k represents the set of quantum numbers characterizing an eigenstate).

We now consider the optical transition of one-photon emission/absorption process between an initial electron-photon state, $|\psi_{k_j}, n_{ph}+1\rangle$, where n_{ph} is the photon density. The first-order time-dependent perturbation theory gives us the optical transition probability from the initial to the final state by the Fermi golden the

$$\frac{2\pi}{\hbar}|\langle\psi_{k_j}, n_{ph}+1|H'|\psi_{k_i}, n_{ph}\rangle|^2\delta(E_{k_i} - E_{k_j} - \hbar\omega). \tag{4}$$

Received 2002 - 09 - 02, revised 2003 - 08 - 18

稿件收到日期 2002 - 09 - 02, 修改稿收到日期 2003 - 08 - 18

Since the vector potential of the electromagnetic field is written as

$$\boldsymbol{A} = \sqrt{\frac{\hbar}{2\omega\varepsilon}}(b^{+} + b), \tag{5}$$

where $\mathbf{b}^{+}$ and $\mathbf{b}$ are photon creation and annihilation operators, it is easy to obtain

$$\langle \psi_{k_j}, n_{ph}+1 \mid \boldsymbol{A}\cdot\nabla \mid \psi_{k_i}, n_{ph}\rangle = \sqrt{\frac{\hbar(n_{ph}+1)}{2\omega\epsilon}}\langle \psi_{k_j} \mid a\cdot\nabla \mid \psi_{k_i}\rangle, \tag{6}$$

where a is the polarization unit vector of the electromagnetic field.

The rate to emit a photon at $\hbar\omega$ is

$$W_{k_jk_i}(\hbar\omega) = \frac{\pi\hbar^2e^2(n_{ph}+1)}{m_0^{\,2}\omega\epsilon} \mid \langle \psi_{k_j} \mid a\cdot\nabla \mid \psi_{k_i}\rangle \mid^2 \delta(E_{k_i} - E_{k_j} - \hbar\omega). \tag{7}$$

from electron state ψ_{k_i} to state ψ_{k_i}.

At the same time, optical absorption is expected

$$W_{k_jk_i}(\hbar\omega) = \frac{\pi\hbar^2e^2n_{ph}}{m_0^{\,2}\omega\epsilon} \mid \langle \psi_{k_i} \mid a\cdot\nabla \mid \psi_{k_j}\rangle \mid^2 \delta(E_{k_j} - E_{k_i} + \hbar\omega), \tag{8}$$

from state ψ_{k_i} to state ψ_{k_i} by absorbing one photon.

The total transition rate from electron state ψ_{k_i} to state ψ_{k_i} is

$$W_{k_ik_j}(\hbar\omega) = W_{k_jk_i}(\hbar\omega)f(E_{k_i})[1 - f(E_{k_j})] - W_{k_jk_j}(\hbar\omega)f(E_{k_j})[1 - f(E_{k_i})], \tag{9}$$

by including the Pauli exclusion principle, i. e., an electron is capable of transiting from an occupied state ψ_{k_i} to an empty state ψ_{k_j}.

At equilibrium status, the occupation of electron state E is expressed by the Fermi function

$$f(E) = \frac{1}{1 + \exp(\dfrac{E - E_f}{\kappa_B T})}, \tag{10}$$

where E_f is the Fermi level.

Normally $n_{ph} \gg 1$. Moreover, $W_{k_ik_j} = W_{k_jk_i}$ so that

$$W_{k_jk_i}(\hbar\omega) = W_{k_jk_i}(\hbar\omega)[f(E_{k_i}) - f(E_{k_j})]. \tag{11}$$

The summation over all possible electron states gives us the total optical transition rate

$$W(\hbar\omega) = \sum_{k_jk_i} W_{k_jk_i}(\hbar\omega). \tag{12}$$

We now relate the optical gain (laser action) and absorption (detection action) coefficients to the optical transition rate. When we consider a beam of photons travelling along the *z-axis*, we can write a continuity equation for the photon density as

$$\frac{dn_{ph}(\hbar\omega)}{dt} = \frac{\partial n_{ph}(\hbar\omega)}{\partial t} - \frac{\partial[cn_{ph}(\hbar\omega)]}{\partial z}, \tag{13}$$

where, on the right side of the equality, the first term represents the net gain/absorption rate of photons,

$$\frac{\partial n_{ph}(\hbar\omega)}{\partial t} = W(\hbar\omega), \tag{14}$$

and the second term describes photons leaving the region between z and $(z+dz)$ due to the photon propagation.

Here c is the velocity of light in the medium. At steady state, $dn_{ph}/dt = 0$, so that Eq. (13) becomes

$$0 = W(\hbar\omega) - \frac{\partial[cn_{ph}(\hbar\omega)]}{\partial z}, \tag{15}$$

having a solution of

$$n_{ph}(\hbar\omega, z) = n_{ph}(\hbar\omega, 0)e^{g(\hbar\omega)z}. \tag{16}$$

which defines the gain/absorption coefficient $g(\hbar\omega)$

$$g(\hbar\omega) = \sum_{k_jk_i} \frac{\pi\hbar^2e^2}{m_0^{\,2}c\omega\varepsilon} \mid \langle \psi_{k_j} \mid a\cdot\nabla \mid \psi_{k_i}\rangle \mid^2 \delta(E_{k_i} - E_{k_i} + \hbar\omega)[f(E_{k_i}) - f(E_{k_j})]. \tag{17}$$

It is thus noticed by Eqs. (16,17) that when $g(\hbar\omega) > 0$, the intensity of the incident radiation becomes amplified, light emission action is expected; Otherwise, if $g(\hbar\omega) < 0$, the radiation intensity reduces along its transmission through the medium, i. e., the radiation becomes absorbed (an absorption coefficient is normally defined as $\alpha = -g$ when $g < 0$).

It is concluded by Eq. (17) that the population inversion, $f(E_{k_i}) > f(E_{k_j})$ when $E_{k_i} > E_{k_j}$, is essential in the generation/amplification of a radiation, whereas at equilibrium status, $f(E_{k_i}) < f(E_{k_j})$ when $E_{k_i} > E_{k_j}$.

2 Numerical Analysis and Discussions

We now discuss low-dimensional InAs model systems embedded between p^{-} and n-GaAs lavers. The low-dimensional systems under investigation are quantum dot, wire and well, which are described mathematically as $L_x \times L_y \times L_z$, $L_x \times L_y$, and L_x. It is further assumed that the InAs model systems are strained so that its energy band gap becomes 1.2eV[7]. The effective masses of the conduction-band electron and valence-band heavy hole are $0.0239m_0$ and $0.35m_0$[8], respectively, where m_0 is the free electron mass (light hole is not directly relevant in low-dimensional systems concerning radiation emission).

At forward bias, both the electrons and holes are injected into the narrow-bandgap InAs region for the required population inversion. The electron and hole densities, n and p, are identical in the InAs active layer. We further assume that the injected carriers are at thermal equilibrium status which is described by the Fermi distribution function. The Fermi levels are determined by

$$n = \frac{1}{L^3}\sum_i \frac{1}{1 + \exp(\dfrac{E_i - E_f^{\,0}}{\kappa_B T})}$$

$$n = \frac{1}{L^2}\sum_i \int \frac{2d\kappa}{2\pi} \frac{1}{1 + \exp(\dfrac{E_i + E_\kappa - E_f^{\,1}}{\kappa_B T})}$$

$$n = \frac{1}{L}\sum_i \int \frac{2d\kappa}{(2\pi)^2} \frac{1}{1 + \exp\left(\frac{E_i + E_\kappa - E_f^2}{\kappa_B T}\right)}. \quad (18)$$

where E_i denotes the energy sublevel due to the quantum confinement. $E_f^{0,1,2}$ denotes the Fermi level in the 0-, 1-, and 2-dimensionally extended system. The quantum dot is three-dimensionally confined (0-dimensionally extended), the quantum wire is 1-dimensionally extended and k is the wave vector along this extended direction, and finally, the quantum well is 2-dimensionally extended and k is the wave vector in this extended plane (for more detail, see[5]). By assuming spherical and parabolic dispersion relationship of

$$E_k = \frac{\hbar^2 k^2}{2m^*}. \quad (19)$$

where m^* is the effective mass, and by assuming $L_x = L_y = Lz = L$ for simplicity, we have calculated the Fermilevels in quantum dot, wire and well as functions of the electron density and the results are presented in Fig. 1. The three-dimensionally-extended system (bulk) is presented for comparison. As would be expected, the Fermi level converges to the one of the bulk material when L increases, and the occupation of high-energy states is clearly reflected (especially in the quantum dot when L is small), which appear as steps in the $E_f - n$ relationship. The steps are due to the fact that the Fermi level locates between the highest occupied state and the lowest empty state. When the carrier density is increased to such a value that one more state becomes occupied, the Fermi level jumps from below the state to above the state. The jump is still significant in the quantum wire, it is however replaced by a slight increase in the slope in the quantum well system due to the much enhanced density of states of two-dimensional continuum states described by k.

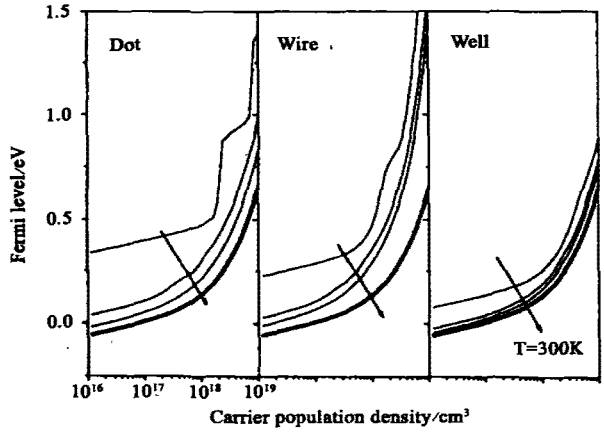

Fig. 1 Fermi levels as functions of concentration of injected carriers. The thicker lines correspond to the bulk material. Arrow indicates the increase of L (100, 200, 400 Å)

Similar results about the Fermi levels of heavy holes in the valence band are obtained.

Knowing the carrier distributions, we now calculate the optical spectrum of Eq. (17). Typical results are presented in Fig. 2. The optical spectrum in general consists of (1) an optical transparent region when the photon energy is smaller than the energy band gap of the system, (2) an optical gain regime, and (3) an optical absorption in the short wavelength regime. The energy band gap of the low-dimensional system is defined as the energy band gap of the InAs bulk material plus the energies of the ground states of electron and heavy hole measured respectively from the conduction- and valenceband-edges.

Moreover, the optical coefficient decreases following the decrease of the optical wavelength, especially in the 2D system where the density of states is in the form of staircase. This is due to the factor of $1/\hbar\omega$ in Eq. (17).

The optical gain is obtained due to the population inversion in the vicinity of the Fermi levels, while the short wavelength region corresponds to transitions between high-electron-energy states and high-hole-energy states. The high-electron-energy states are not populated by electrons when the electron energies are higher than the electron Fermi level, i. e., $f(E_{k_i}) \to 0$ when $E_{k_i} > E_f$. Similarly, the high-hole-energy states are not occupied by holes, it is occupied by electrons so that $f(E_{k_j}) \to 1$. Population inversion requirement is thus not fulfilled in this short wavelength region, so that $g(\hbar\omega) < 0$ (optical absorption). In the infrared region, optical absorption is obtained due to the intra-band optical transition (the results are not presented).

The effect of the population inversion is further elucidated by Fig. 2 when increasing the concentrations of electrons in the conduction band and holes in the valence band. With a carrier density of $1 \times 10^{18}\,\mathrm{cm}^{-3}$, we obtain optical gains in 1D, 2D and 3D systems, while the optical coefficient $g(\hbar\omega)$ of system 0D is negative in the whole optical wavelength region under investigation. It is noticed that the density of states of the 0D system is $2/L^3$ at each energy level, where the factor of 2 accounts for the spin degeneracy. It is $2 \times$

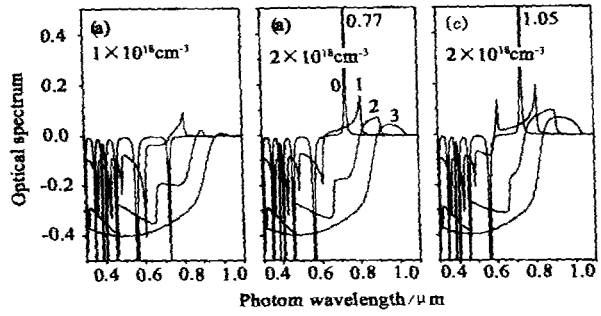

Fig. 2 Optical spectra of low-dimensional systems. L = 100Å, T = 300K. Integer 0, 1, 2, and 3 indicate the dimensionality of the system. Numerical values on the right sides of the highest peaks peaks in (b) and (c) are the peak intensities

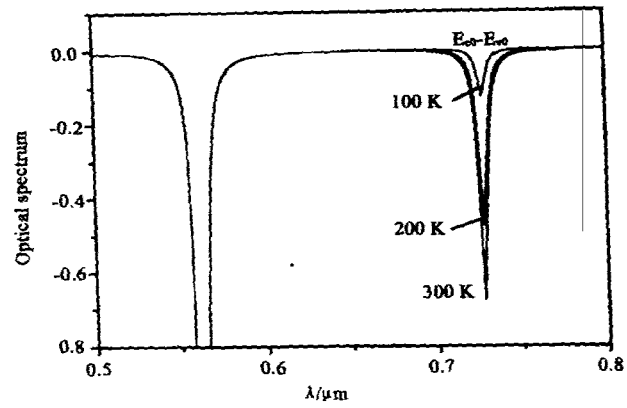

Fig. 3 The optical spectrum of a quantum dot system as a function of the device temperature. L = 100Å and $n = 1 \times 10^{18}\,\mathrm{cm}^{-3}$

$10^{18}\,\mathrm{cm}^{-3}$ when L = 100Å. The ground levels (electron and hole) are thus only half occupied when the injected carrier density is $1 \times 10^{18}\,\mathrm{cm}^{-3}$ at zero temperature, i.e, $f(E_{c0}) = f(E_{v0}) = 0.5$ so that the optical coefficient $g(\hbar\omega) = 0$ at $\hbar\omega = E_{c0} - E_{v0}$, where E_{c0} and E_{v0} are ground states of electron and hole in the quantum dot. At room temperature we expect thermal excitation so that the occupation of the ground levels are less than 0.5. The thermal excitation of the holes in the valence band are more intensive than the one of electrons due to the small energy separations between energy states (large hole effective mass), so that the population inversion between the two ground levels is not established, resulting in a negative optical coefficient. The physical phenomenon is demonstrated in Fig. 3.

A threshold value for the population inversion is thus concluded in the quantum dot system for optical gain, namely, two energy states must be more than half occupied before the optical coefficient of the transition between the two states becomes positive (optical gain).

Another striking feature in Fig. 2 is about the peaks corresponding to the energy sublevels in the low-dimensional systems and the peak lineshapes corresponding to the dimensionality-dependent densities of states[5].

The optical transparency ($g(\hbar\omega) = 0$) in the long wavelength region is normally expected when the photon energy is smaller than the energy band gap, simply because there is no carrier available to interact with photons. However, close investigation in this transparency region reveals that below the energy band gap, $g(\hbar\omega) < 0$. The problem was discussed by Coldren and Corzine in the context of the lineshape broadening[9], that the delta function in Eq. (17), which is due to the energy conservation, must be replaced by

$$\frac{\Gamma}{(E_{k_j} - E_{k_i} + \hbar\omega)^2 + \Gamma^2}, \tag{20}$$

or other forms to include energy relaxation processes [10-14], where $\hbar/\Gamma$ is the lifetime of carrier, which is about 0.1 ps(Γ = 6.6meV). When $\hbar\omega < E_g - 10\Gamma$,

$$\frac{\Gamma}{(E_{k_j} - E_{k_i} + \hbar\omega)^2 + \Gamma^2} \approx \frac{\Gamma}{(E_{k_j} - E_{k_i} + \hbar\omega)^2}. \tag{21}$$

which varies slowly with carrier's energy. $g(\hbar\omega)$ becomes negative after the performance of the integration in Eq. (17) over k_i and k_j, since the population inversion occurs only near the conduction-and valence-band edges. The optical absorption rate reduces when the dimensionality of the system is reduced due to the in-

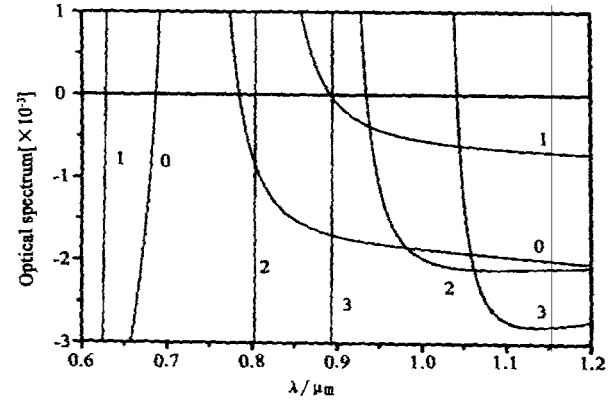

Fig. 4 Same as Fig. 2b but in a different plot window

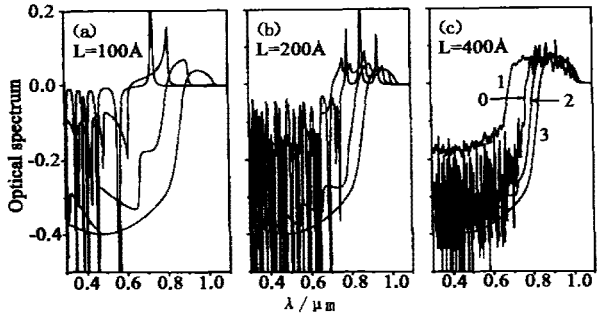

Fig. 5 Optical spectra of low-dimensional systems as functions of the system size L. $n = 3 \times 10^{18}\,\mathrm{cm}^{-3}$. $T = 300\mathrm{K}$

creased energy band gap, as clearly demonstrated by Fig. 4. The anomalous increase of the optical absorption in the quantum dot is due to its unique delta-formed density of states, whereas extended states exist in other systems.

On the other band, when $\Gamma \to 0$, $g(\hbar\omega) \to 0$ when $\hbar\omega < E_g$, resulting in a complete optical transparency. However, an infinitely-long lifetime of carrier is not physical.

The effect of the size of the low-dimensional system is presented in Fig. 5, showing that the optical spectra of low-dimensional systems approach the one of bulk material as L increases.

3 Summary

We have studied the optical properties of low-dimensional systems by theoretically calculating the complete optical spectra. The optical spectrum in general consists of an optical transparent, an optical gain, and an optical absorption regime. Reducing the dimensionality of the system improves the intensities and symmetries of the peaks.

It is found that due to the uniqueness in the density of energy states of the quantum dots, a threshold population inversion exists for optical gain.

REFERENCES

[1] Nalwa H S. *Handbook of Advanced Electronic and Photonic Materials and Devices*. San Diego: Academic Press San Diego, 2000

[2] Kim S, Razeghi M. Chapter 3 Recent advances in quantum dot optoelectronic devices and future trends, Nalwa H S, In *Handbook of Advanced Electronic and Photonic Materials and Devices*. San Diego: Academic Press San Diego 2000, **2**: 133—154

[3] Gunapala S D, Liu J K, Park J S. *et al*. 9 – μm cutoff 256 * 256 GaAs/$Al_xGa_{1-x}As$ quantum well infrared photodetector hand-held camera. *IEEE. Trans. Electron Dvices*, 1997, **44**: 51—57

[4] Asada M, Miyamoto Y, Suematsu Y. Gain and the threshold of three-dimensional quantum-box lasers, *J. Quantum Electronics*, 1986, **22**: 1915—1921

[5] Fu Y, Willander M, Li Z F. *et al*. Dimensionality of photoluminescence spectrum of GaAs/AlGaAs system. *J. Appl. Phys*, 2001, **89**: 5112—5116

[6] Fu Y, Willander M, Xu Wenlan. Optical absorption coefficients of semiconductor quantum-well infrared detectors. *J. Appl. Phys*, 1995, **77**: 4648—4654

[7] Fu Y, Zhao Q X, Ferdos F, *et al*. Strain and optical transitions in InAs quantum dots on (001) GaAs. Superlattices and Microstructures, 2001, **30**: 205—213

[8] Madelung O. *Semiconductors Group IV Elements and* Ⅲ-Ⅴ *Compounds*. Berlin: Springer-Verlag, 1991, 134

[9] Coldren L A, Corzine S W. *Diode Lasers and Photonic Integrated Circuits*. New York: John Wiley & Sons Inc. 1995, 130

[10] Yamada M, Ishiguro H. Gain calculation of undoped GaAs injection laser taking into account of electron intra-band relaxation, *Jpn. J. Appl. Phys.*, 1981, **20**: 1279—1288

[11] Yamanishi M, Lee Y. Phase dampings of optical dipole moments and gain spectra in semiconductor lasers. *IEEE J. Quantum Electronics*, 1987, **23**: 367—370

[12] Chinn S R, Zory P, Reisinger A R. A model for GRIN-SCH-SQW diode lasers. *IEEE J. Quantum Electronics*, 1988, **24**: 2191—2194

[13] Kucharska A I, Robbins D J. Lifetime broadening in GaAs-AlGaAs quantum well lasers. *IEEE J. Quantum* Electronics, 1990, **26**: 443—448

[14] Asada M. *Chapter 2 Intraband relaxation effect on optical spectra*, In P. S. Zory *Quantum Well Lasers*. Jr., San Diego: Academic Press San Diego, 1993